Ultrafast Internal Conversion in Highly Excited Toluene Monomers and Dimers†

P. Farmanara, V. Stert, W. Radloff,* and I. V. Hertel‡

Max-Born-Institut für Nichtlineare Optik und Kurzzeitspektroskopie, Max-Born-Str. 2A, D-12489 Berlin, Germany

Received: October 18, 2000; In Final Form: February 1, 2001

The dynamics of the internal conversion in toluene molecules and dimers excited to the electronic S_2 state by 150 fs laser pulses at 202 nm has been studied in pump−probe experiments by detection of the ions and the coincident photoelectrons. The time-dependent ion signals reflect an ultrafast (∼50 fs) internal conversion from the excited S_2 state down to the lower electronic S_1 and S_0 states for the monomer as well as the dimer. The decay of the secondarily populated S_1 state proceeds within 4.3 ps for the toluene molecule and more than 100 ps for the dimer. The energy distribution of the photoelectron spectra for the monomer and the dimer ion demonstrate the significant geometry differences between the corresponding electronic states included in the processes of excitation, ionization and relaxation. The structure of the photoelectron spectra measured at simultaneous absorption of the pump and probe photons is tentatively assigned to vibrational modes of the ion states. The comparison of the electron spectra before and after the internal conversion out of the S_2 state directly reflects the growth of the vibrational energy in the secondarily populated S_1 states of the toluene monomer and dimer.

1. Introduction

In polyatomic molecules and molecular clusters excited to higher electronic states, internal conversion (IC) to vibronic levels of lower electronic states is one of the dominant mechanisms for deactivation. As a prototype molecule, benzene has been studied for many years in great detail by the group of E. Schlag (see e.g., ref 1). Here, higher vibrational levels of the S_1 electronic state (in the channel three region) as well as S_2 state levels are deactivated very rapidly by IC. The dynamics of this process in aromatic molecules (e.g., benzene and pyrazine) has been discussed theoretically on a microscopic level in terms of a conical intersection of the respective potential energy surfaces within the Franck−Condon region. Experimentally, the dynamics of internal conversion and the change of the internal energy during this process have been analyzed by photoelectron spectroscopy for a few isolated molecules of a somewhat more complex structure, for example, 1,3,5-hexatriene[4] and decatetraene.[5]

Recently, we have studied the dynamics of IC in the benzene monomer and dimer in a femtosecond pump−probe experiment. The S_2 electronic state is excited by laser pulses at 200 nm and probed at 267 nm by ionization.[6] The analysis of the time-dependent ion signals obtained gives lifetimes of about 40 fs for both, the benzene monomer and dimer. The decay process is attributed to IC from the S_2 state to higher vibrational levels of the S_1 and the S_0 state, the former process being the dominant mechanism. In contrast, the S_2 to S_1 transition occurs only with a very small branching ratio of 1% and 2.3% for the benzene monomer and dimer, respectively. This has been estimated from the relative strengths of the ion signals at longer delay times, the S_1 state being depopulated with a time constant of 6.7 ps, and 100−200 ps for the monomer and dimer, respectively.[6] Equal ionization efficiencies were assumed for the S_2 and the S_1 state in both species, an assumption which appears justified in view of the broad Franck−Condon regions found for the corresponding transitions[7] implying an only weak dependence of the transition probabilities on the different levels of vibrational excitation.

The femtosecond time-resolved photoelectron spectroscopy developed and applied by us for the analysis of clusters has allowed us to follow directly the time evolution of the internal cluster energy distribution during the internal conversion processes in the benzene monomer and dimer.[7] Relatively broad electron spectra are observed in this case immediately after excitation (zero delay time between pump and probe pulse), while already after a few 100 fs, the energy distribution is narrowed and concentrated on low electron kinetic energies only—reflecting the increase of the internal energy in the monomer and dimer due to IC. Surprisingly, despite of the high internal energy, contained in the neutral and in the ionic state after the internal conversion, which is significantly larger than the binding energy of the benzene dimer, no fragmentation has been observed. Apparently, the S_2 to S_1 state conversion leads to a stable combination of excited intramolecular vibrations in the S_1 state of the dimer (and after ionization in the ionic state). The energy transfer to intermolecular vibrations in the benzene dimer ion appears to be rather inefficient so that fragmentation on a time scale of some 100 ns (the time spent by the ions in the extraction region of the mass spectrometer) does not occur.

In the present paper, we report a study on the corresponding processes in toluene and toluene dimers as an example of a system with strongly reduced symmetry (no D_{6h} symmetry). The nondegeneracy of states in this benzene derivative leads to a higher density of the vibrational levels and to a reduction of symmetry-forbidden interactions. Hence, higher coupling rates for nonadiabatic transitions are expected. Again, we use femtosecond pump−probe techniques and time-resolved photo-

† Part of the special issue "Edward W. Schlag Festschrift".

* To whom correspondence should be addressed. E-mail: Radloff@mbi-berlin.de

‡ Also at Fachbereich Physik, Freie Universität Berlin, Arnimallee 14, D-14195 Berlin, Germany.

10.1021/jp003818f CCC: $20.00
Published on Web 03/23/2001

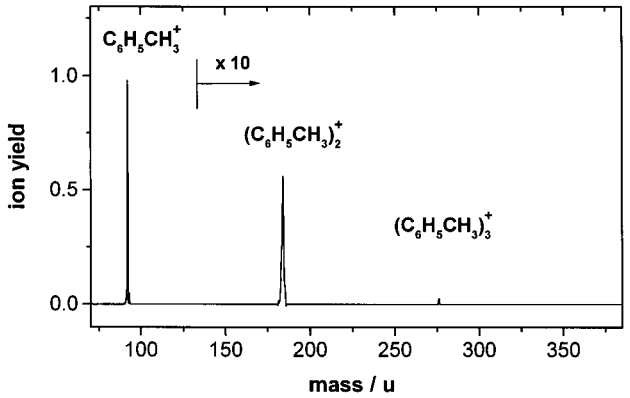

Figure 1. Typical mass spectrum of toluene clusters, indicating only a small fraction of clusters with $n > 2$.

electron photoion coincidence spectroscopy (fs-PEPICO). The toluene monomer and dimer are excited by pump photons with an energy of 6.14 eV (wavelength 202 nm), which exceeds the energies of the S_1 and the S_2 electronic states.

2. Experimental Section

The toluene molecules and clusters are cooled in a supersonic molecular beam by adiabatic expansion of toluene (0.16%) seeded in He gas (1.2 bar) through a pulsed nozzle. At such low concentration, the cluster size distribution is restricted mainly to small cluster masses. This is documented in a typical mass spectrum shown in Figure 1.

After passing a skimmer (1 mm), the molecular beam interacts with the femtosecond laser pulses of two weakly focused copropagating laser beams. The molecules and clusters are excited with a pump pulse (wavelength 202 nm) and ionized by a probe pulse (wavelength 269 nm) delayed by the time τ with respect to the pump pulse. The ions are detected by a Wiley−McLaren time-of-flight mass spectrometer while the coincident photoelectrons are analyzed by a time-of-flight "magnetic bottle" electron spectrometer. The ion and electron signals detected by microchannel plate detectors are registered in a multihit time-to-digital converter (Le Croy 4208) started by the laser pulses.[8]

The laser system used is a commercial Ti-sapphire laser and amplifier system (Clark MXR) tuned to 808 nm. The pulsed laser beam is split into two parts, one of which is transformed to the fourth harmonic by three successive BBO crystals (pump), while the second part is frequency tripled by two additional BBO crystals (probe).[9] The width τ_L (FWHM) of the laser pulses is about 150 fs. For the electron spectroscopy (fs-PEPICO), the laser fluences have to be reduced strongly to ensure ionization rates significantly below 1 per laser pulse so that accidental coincidences are suppressed. Typically, we use 20μJ/cm^2 for the pump and 500μJ/cm^2 for the probe pulse. With these fluences, we obtain total coincidence rates below 0.1 per laser pulse, so that uncorrelated coincidences remain below 10%.[8] Hence, at a pulse repetition frequency of 1 kHz a data acquisition time of 1 h is needed to accumulate about $4 \cdot 10^5$ coincidences.

3. Results and Discussion

Figure 2 shows the energy scheme of the ground, excited and ionic states of toluene monomer involved in the present pump−probe study. The pump photon energy $h\nu_1$ exceeds the energies of the S_1 and the S_2 electronic states. In contrast to the term energy of the S_1 state (4.647 eV, vibrationless $S_0 \rightarrow S_1$ transition[10]), the position of the S_2 state is not exactly known

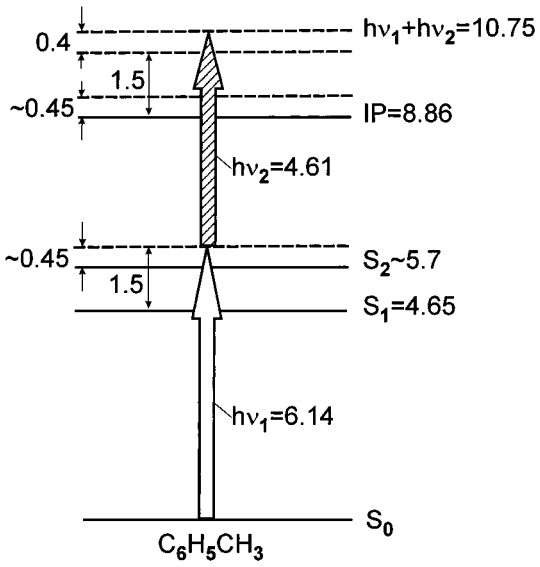

Figure 2. Energy scheme of the toluene monomer (all quantities in eV). The energies of the pump ($h\nu_1$) and the probe ($h\nu_2$) photons are drawn in scale.

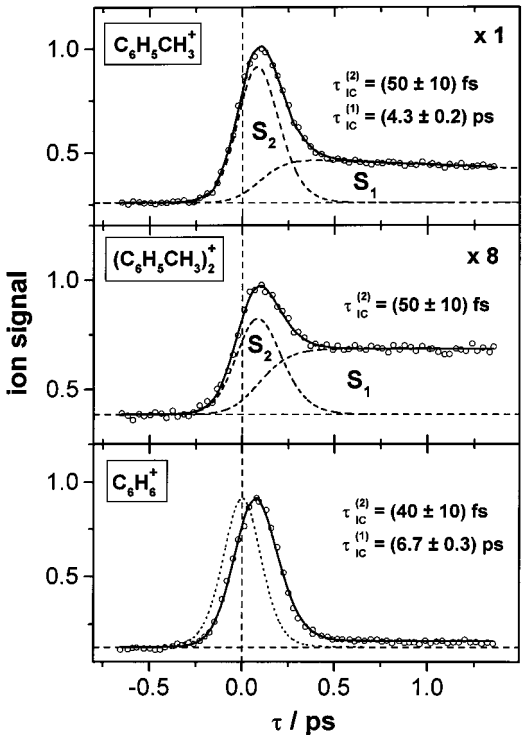

Figure 3. Ion signals of the toluene monomer and dimer as a function of the delay time τ between the pump (202 nm) and probe (269 nm) pulses. The signals are superimposed by two contributions (S_2) and (S_1) with decay times $\tau_{IC}^{(2)}$ and $\tau_{IC}^{(1)}$ (see text). The numbers in the upper right corner denote the magnification factors for the different ion signals. Below, for comparison, the time-dependent benzene ion signal is given along with the cross correlation curve of the laser pulses (dotted line).

and has been estimated by the measured absorption spectrum.[11] For the dimer, the $S_0 \rightarrow S_1$ (0−0) transition energy is about 4.58 eV and the ionization potential is 8.34 eV.[12] The probe photon energy $h\nu_2 = 4.61$ eV is below (for the monomer) or close to (for the dimer) the S_1 state energy, thus avoiding any significant signal due to ionization with the pump photon (i.e., at negative delay times τ).

Figure 3 shows the time-dependent ion signals for the toluene monomer and dimer as determined by the pump−probe experi-

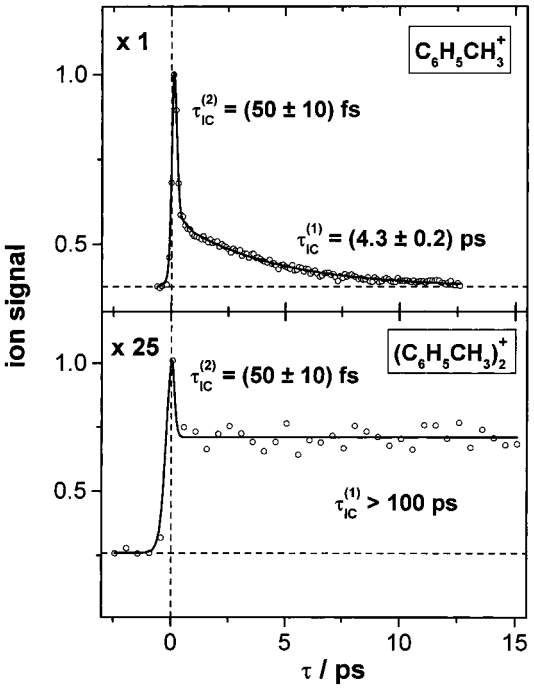

Figure 4. Ion signals of the toluene monomer and dimer for longer delay times τ between the pump and probe pulses. Otherwise, they are as Figure 3.

ment and a comparison with benzene. The observed time dependence can be interpreted by the superposition of two contributions: one part (S_2) reflects the excitation and decay of the initially excited S_2 state and the other part (S_1) is due to the population of the S_1 state. The first contribution is fitted within our model of optical Bloch equations,[13] which describe the resonant coherent excitation of the S_2 state by the pump pulse followed by a single-exponential decay with a time constant $\tau_{IC}^{(2)}$. The second contribution, which builds up with $\tau_{IC}^{(2)}$ and decays with the time constant $\tau_{IC}^{(1)}$ can be described by a simple rate equation. As a result of a least-squares fit, we obtain an S_2 state lifetime $\tau_{IC}^{(2)} = 50 \pm 10$ femtosecond for both the monomer and the dimer. It is again attributed to IC down to the S_1 and S_0 state in both cases. This accuracy of the measured lifetime $\tau_{IC}^{(2)}$ relies on an exact determination of the zero delay time between pump and probe pulse by comparison with the simultaneously measured benzene signal. That, in turn has been calibrated in earlier experiments. The extremely large IC rates for both the toluene molecule and dimer are again attributed to conical intersections of the corresponding potential energy surfaces (apparently unaffected by intermolecular effects in the dimer)—in close analogy to the benzene system.[2,3] A quantitative interpretation of these observations constitutes a major challenge for future theoretical work.

From extended delay scans, as shown in Figure 4, we can also derive the lifetime of the product state S_1, which is much longer: $\tau_{IC}^{(1)} = (4.3 \pm 0.2)$ ps for the monomer and $\tau_{IC}^{(1)} > 100$ ps for the dimer. IC to the S_0 state is held responsible for this decay. Assuming, as in the benzene case (see the Introduction), nearly equal ionization efficiencies for the S_2 and the S_1 state, we can estimate the branching ratio for $S_2 \rightarrow S_1$ state conversion to be ~30% for the toluene monomer and ~70% for the dimer. These branching ratios are about 30 times larger than the corresponding ones for benzene. Whereas for the benzene monomer and dimer $S_2 \rightarrow S_0$ internal conversion is the dominant decay channel, for toluene, the $S_2 \rightarrow S_1$ IC-rate state is of the same order of magnitude. Most likely, this is caused by the

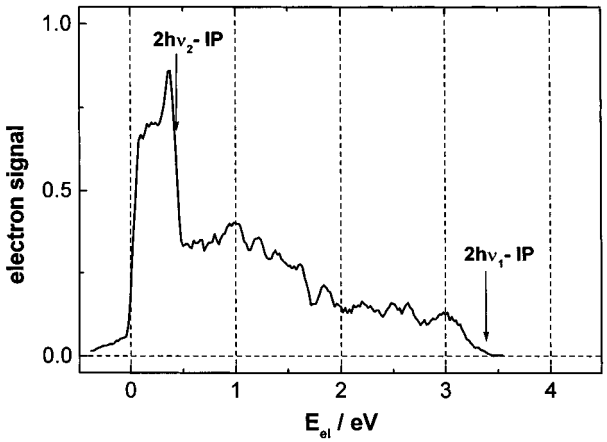

Figure 5. Electron spectrum of the toluene ion measured at the delay time $\tau = -1$ ps. The arrows denote the maximum electron energies E_{el}^{max} for the absorption of two probe ($h\nu_2$) and two pump ($h\nu_1$) photons, respectively.

higher density of vibrational levels in the S_1 state of toluene which couple by nonadiabatic interaction to the levels of the excited S_2 state. In contrast, the lifetimes of both, the S_2 and S_1 states of the toluene monomer and dimer are roughly the same as the corresponding lifetimes in benzene.

Turning now to the results of the photoelectron spectroscopy, we discuss at first the background signal for the toluene monomer (measured at a pump−probe delay $\tau = -1$ ps). Figure 5 shows two sharp edges at electron kinetic energies $E_{el} = 0.45$ eV and $E_{el} = 3.4$ eV which correspond to the maximum expected for absorption of two probe photons ($E_{el} = 2h\nu_2 - IP$) and two pump photons ($E_{el} = 2h\nu_1 - IP$), respectively.

Figure 6 shows the femtosecond-PEPICO electron spectra for the toluene molecule at pump−probe delay times $\tau = 0.1$ ps (a) and $\tau = 1$ ps (b). The background signal has been subtracted in both cases. The maximum electron signal (and ion signal, see Figure 3) is obtained at $\tau = 0.1$ ps. Here, the signal is dominated by the S_2 contribution, i.e., by ionization of molecules which are still in the initially excited S_2 state. However, as already documented in Figure 3, a small fraction of about 15% has already undergone IC to the S_1 state and gives rise to an enhanced signal at low electron kinetic energies.

The distribution of this additional part in Figure 6a is identical to the energy spectrum at $\tau = 1$ ps where all toluene molecules are either in the S_1 state (cf. Figure 6b) or in the S_0 ground state from where they cannot be ionized.

By scaling the distribution shown in Figure 6b according to the ratio between S_1 and S_2 population derived from the ion signal Figure 3, we can subtract the S_1 contribution from the signal shown in Figure 6a to obtain the pure S_2 electron spectrum (thin line in Figure 6a). This relatively flat distribution reflects a broad $S_2 \rightarrow$ *ion* Franck−Condon region. Vibrational energies in the ion (E_{vib}) range from zero (at $E_{el} = E_{el}^{max}$) up to the maximum possible value of $E_{vib}^{max} = h\nu_1 + h\nu_2 - IP = 1.9$ eV ($E_{el} = 0$), with a maximum in the distribution at around 0.5 eV ($E_{el} = 1.4$ eV) which appears to reflect a (weak) propensity rule $\Delta v \simeq 0$, the vibrational energy in the excited S_2 state being 0.45 eV (cf. Figure 2).

It is interesting to note that the structure on the electron spectrum Figure 6a appears to represent a vibrational progression with an energy spacing of 0.19 eV. Tentatively, this progression is assigned to the υ_8 bending mode of toluene in the ionic ground state. As well-known, the υ_8 mode dominates the spectrum of the S_2 state of benzene because it is the active mode for the

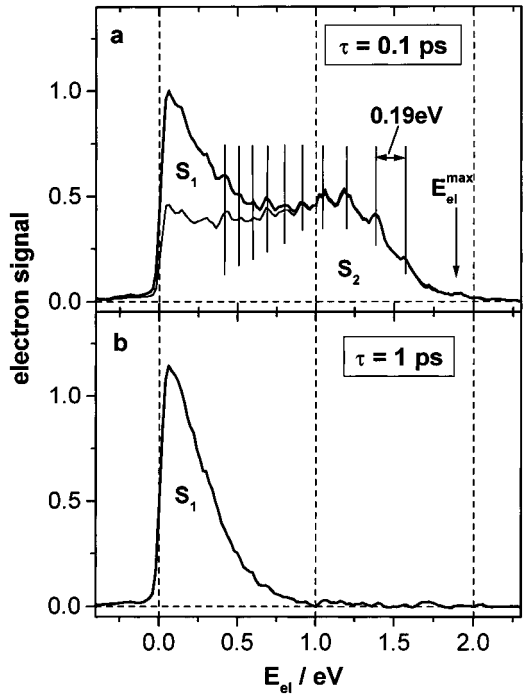

Figure 6. Electron spectra of the toluene monomer ion for delay times $\tau = +0.1$ ps (a) and $\tau = +1$ ps (b). Spectrum (a) extends up to the maximum energy $E_{el}^{max} = 1.9$ eV and contains a small contribution from S_1 in addition to major component arising from S_2 ionization (thin line). The structure on top of the spectrum is attributed to the vibrational progression of the ν_8 bending mode. Spectrum (b) arises from ionizating the S_1 state after the internal conversion from S_2.

pseudo-Jahn−Teller $S_2 \rightarrow S_3$ coupling, leading to a remarkable change of the benzene geometry in the S_2 state.[14] It should be important also in the toluene system. In contrast to benzene, here, the ν_8 progression will also exist for the ion state of toluene due to the lower symmetry of this molecule compared to benzene. In benzene, this mode is degenerate (e_{2g}), in toluene the component ν_{8a} is totally symmetric allowing a progression with $\Delta\nu_8 = 0, \pm1, \pm2, \pm3, ...$ in the ion. In the electronic ground state the corresponding frequency is $\nu_{8a} = 1605$ cm^{-1} (0.199 eV).[15] Assuming a nearly equal value also for the toluene ion the observed separation of 0.19 eV in the progression seen in Figure 6a is very plausible.

The electron spectrum for the longer delay time $\tau = 1$ ps (Figure 6b) reflects the IC from the excited electronic S_2 state to the S_1 state which after 1 ps is complete. IC leads to high vibrational energy in the S_1 state of up to 1.5 eV (cf. Figure 2). Assuming similar geometries in the neutral S_1 state and in the ionic ground-state we expect comparable vibrational excitation (propensity rule) also in the latter leading to electron energies up to about 0.4 eV. The observed electron spectrum shown in Figure 6b displays only a relatively small tail at energies $E_{el} = 0.4$ eV, thus confirming this line of arguments. On the other hand, the electron signal peaks at $E_{el} \simeq 0$ (vibrational energy $\simeq 1.9$ eV) reflecting a certain difference between the geometries of the S_1 state and the ionic ground state.

In Figure 7 the electron spectra for the toluene dimer are displayed at three different pump−probe delay times τ. In the top panel (a) the background spectrum detected at $\tau = -1$ ps is shown to be concentrated on the interval between $E_{el} = 0$ to 0.85 eV. The latter value corresponds to $2h\nu_2 - IP$, thus, this background signal is due to absorption of two probe photons. The small, nearly constant contribution up to energies above 2.6 eV is caused by absorption of two pump photons. There is, however, no noticeable contribution from exciting the dimer

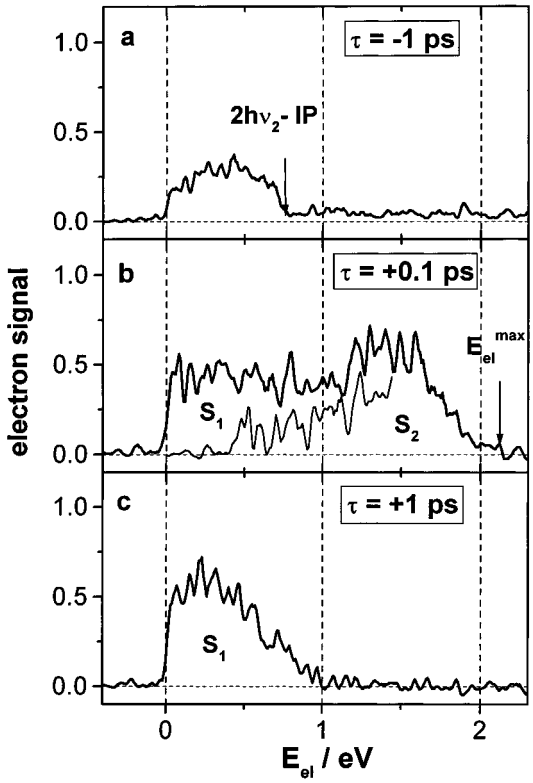

Figure 7. Electron spectra of the toluene dimer ion at delay times $\tau = -1$ ps (a, background), $\tau = +0.1$ ps (b) and $\tau = +1$ ps (c). The main part of the background spectrum (a) extends up to $E_{el}^{max} = 0.85$ eV corresponding to the absorption of two probe photons $h\nu_2$. The background (a) is already subtracted from the electron spectra at $\tau = +0.1$ ps (b) and $\tau = +1$ ps (c). The maximum electron energy of 2.4 eV at $\tau = +0.2$ ps is given by $E_{el}^{max} = h\nu_1 + h\nu_2 - IP$. The vibrational structure is tentatively assigned in the text.

with a probe photon of 4.61 eV and ionizing it with a time-delayed pump photon of 6.14 eV. The complete background signal has been subtracted from the electron spectra for $\tau = +0.1$ ps and $\tau = +1$ ps as represented in Figures 7b,c.

As above, for the toluene monomer, the electron spectrum for the dimer at $\tau = +0.1$ ps reflects preferentially the ionization of the originally excited S_2 state. Here, as determined from Figure 3, about 25% of the signal at low electron energies results from the S_1 state, which is already partially populated at $\tau = +0.1$ ps. At this delay time, the electron spectrum ranges up to nearly the maximum possible electron energy $E_{el}^{max} = h\nu_1 + h\nu_2 - IP$, again a documentation of a broad Franck−Condon region for the $S_2 \rightarrow$ *ion* transition. The observed vibrational progression on top of the electron signal at energies above 1 eV with a distance of about 0.1 eV between adjacent peaks is not yet understood due to the lack of spectroscopic data for the toluene dimer in the neutral excited states and ionic ground state. Clearly, it is due to an intramolecular vibrational mode, possibly a combination band of the ν_8 progression with another mode of about half of the vibrational energy. Such vibrations, allowed only for the dimer ion, are the out-of-plane modes $\nu_4(b_1)$, $\nu_{10a}(a_2)$ and $\nu_{10b}(b_1)$ of toluene in the energy range between 700 and 850 cm^{-1}.[15] Due to symmetry considerations, the simultaneous appearance of two combination bands, characterized by the ν_8 progression ($\Delta\nu_8 = 0, \pm1, \pm2, ..$) and $\Delta\nu = \pm0$ or $\Delta\nu = \pm1$ for the out-of-plane mode, is forbidden for the toluene monomer ion; however, it is allowed for the less symmetric dimer.

At a delay time $\tau = +1$ ps (Figure 6c), the measured electron spectrum exclusively reflects the ionization of the dimer out of the S_1 state, which is populated by internal conversion from

the S_2 state. IC to the S_0 state cannot be detected because at our probe pulse energy the highly excited S_0 state cannot be ionized. According to the energetics (cf. Figure 2), the electron spectrum of the dimer should extend up to $E_{el}^{max} = h\nu_1 + h\nu_2 - IP - E_{int} = 0.85$ eV if the internal energy E_{int} in the ion is equal to the vibrational energy of 1.55 eV in the S_1 state. That is indeed essentially what we observe in Figure 7c. Because of this and the fact that the maximum of the electron signal occurs at energies $E_{el} > 0$, we conclude that the geometries of the neutral S_1 and the ionic ground state of the toluene dimer do not differ very much.

As for the benzene case, a very astonishing result for the toluene dimer is the fact, that its ions do not dissociate despite of a vibrational energy content of up to about 2.4 eV, an energy far above the dissociation threshold in the dimer ion. This result can be understood only by assuming that the high vibrational energies, deposited in the ion state via the S_2 or the S_1 state, are concentrated for long times preferentially in *intra*molecular vibrations. The energy transfer to the *inter*molecular vibrations in the toluene dimer seems to be rather slow so that fragmentation of the ions does not occur during their residence time of a few 100 ns in the extraction region of the mass spectrometer. Comparative experiments with a narrow and a broad cluster distribution in the molecular beam (as realized, e.g., by different seed ratios) do not lead to significantly different electron signal relations. We can thus exclude that the dimer ion signal is obscured by fragmentation of the trimer.

4. Conclusions

We have studied the internal conversion processes of toluene molecules and dimers excited to the electronic S_2 state by 150 fs laser pulses at 202 nm. The analysis of the time-dependent ion signals reveals an ultrafast decay of the primarily excited state down to the lower electronic S_1 and S_0 states within about 50 fs for the monomer as well as for the dimer. The decay of the secondarily populated S_1 state levels proceeds within 4.3 ps for the toluene molecule and more than 100 ps for the dimer. These lifetimes are roughly comparable to the corresponding values for the benzene monomer and dimer. In contrast, however, the branching ratios for the $S_2 \rightarrow S_1$ conversion are much larger for the toluene species than for the benzene system.

The photoelectron spectra reveal broad Franck−Condon regions for the ionization of the toluene monomer and dimer via the S_2 electronic state reflecting significant differences in the geometries of the corresponding electronic states. The discrete structure on the electron spectrum of the toluene ion can be identified as being due to the υ_8 bending mode, whereas for the dimer ion the assignment to a combination band of the υ_8 mode with an out-of-plane mode is only tentative.

For delay times at which internal conversion from the S_2 state is completed, we observed much narrower electron spectra with low photoelectron energies reflecting the increase of the vibrational energy in the terminal S_1 state. Despite of the high internal energy, the toluene dimer does not fragment significantly. Obviously, this energy is preferentially deposited into intramolecular modes that do not couple to the *inter*molecular bond.

Acknowledgment. Financial support by the Deutsche Forschungsgemeinschaft through Sonderforschungsbereich 450 is gratefully acknowledged.

References and Notes

(1) Kiermeier, A.; Ernstberger, B.; Neusser, H. J.; Schlag, E. W. *J. Phys. Chem.* **1988**, *92*, 3785.
(2) Sobolewski, A. L.; Woywod, C.; Domcke, W. *J. Chem. Phys.* **1993**, *98*, 5627.
(3) Seidner, L.; Stock, G.; Domcke, W. *Chem. Phys. Lett.* **1994**, *228*, 665.
(4) Cyr, D. R.; Hayden, C. C. *J. Chem. Phys.* **1996**, *104*, 771.
(5) Blanchet, V.; Zgierski, M. Z.; Seideman, T.; Stolow, A. *Nature* **1999**, *401*, 52.
(6) Radloff, W.; Freudenberg, Th.; Ritze, H.-H.; Stert, V.; Noack, F.; Hertel, I. V. *Chem. Phys. Lett.* **1996**, *261*, 301.
(7) Radloff, W.; Stert, V.; Freudenberg, Th.; Hertel, I. V.; Jouvet, C.; Dedonder-Lardeux, C.; Solgadi, D. *Chem. Phys. Lett.* **1997**, *281*, 20.
(8) Stert, V.; Radloff, W.; Schulz, C. P.; Hertel, I. V. *Eur. Phys. J. D* **1999**, *5*, 97.
(9) Ringling, J.; Kittelmann, O.; Noack, F.; Korn, G.; Squier, J. *Opt. Lett.* **1993**, *18*, 2925.
(10) Geppert, W. D.; Dessent, C. E. H.; Cockett, M. C. R.; Müller-Dethlefs, K. *Chem. Phys. Lett.* **1999**, *303*, 194.
(11) Hippler, H.; Troe, J.; Wendelken, H. J. *J. Chem. Phys.* **1983**, *7*, 5351.
(12) Ernstberger, B.; Krause, H.; Kiermeier, A.; Neusser, H. J. *J. Chem. Phys.* **1990**, *92*, 5285.
(13) Freudenberg, Th.; Radloff, W.; Ritze, H.-H.; Stert, V.; Weyers, K.; Noack, F.; Hertel, I. V. *Z. Phys. D* **1996**, *36*, 349.
(14) Sension, R. J.; Brudzynski, R. J.; Li, S.; Hudson, B. S.; Zerbetto, F.; Zgierski, M. Z. *J. Chem. Phys.* **1992**, *96*, 2617.
(15) Morrison, V. J.; Laposa, J. D. *Spectrochim. Acta A* **1976**, *32*, 443.